Data Assimilation Project II and Project III

Shan Leng

April 2025

1 Introduction

Observational System Similation Experiment (OSSE) is a rigorous and cost-effective way to evaluate and verify the performance of Data Assimilation (DA) strategies by applying the strategies on chaotic toy systems. [3] In this report, a DA method is 3D if the background covariance matrix P^b does not evolve with time, and only background $\vec{x}_b$ changes with time and is assimilated to $\vec{x}_a$. This is considered 3D because only information of background and observational positional vectors $\vec{x}_b$ and $\vec{y}_o$ at the appropriate time is utilized for assimilation. For 4D methods, P^b also evolves with time, and it is assimilated to P^a at the end of the time window. Thus, other than positions of background and observation at appropriate time, for 4D methods, the change of background error covariance along the trajectory in the time window is also estimated to get the analysis. This paper reports results from Optimal Interpolation and EKF on Lorenz 3 System.

2 System of Interest : Lorenz 3 System

This is a chaotic system that was discovered by Edward Lorenz in 1963 while studying atmospheric convection. [4]

$$\begin{cases} \frac{dx}{dt} = \sigma(y-x) \\ \frac{dy}{dt} = x(\rho-z)-y \\ \frac{dz}{dt} = xy-\beta z \end{cases} \tag{1}$$

with $\sigma = 10, \beta = 8/3, \rho = 28$. This system is simulated with $\delta t = 0.01$, which is around 1/100 of the Lyapunov time, using Runge Kutta 4 method.The time window (TW) for all assimilation experiments is chosen to be 0.1, and observation is only taken at the end of each time window.

3 3-D Method : Optimal Interpolation (OI)

3.1 Method Description

This is an approach that minimizes the trace of the P^a by optimally combining background $\vec{x}^b$ and Innovation $\vec{d}^{ob} = \vec{y}^o - H\vec{x}^b$ using Best Linear Unbiased Estimation (BLUE). H is the operator matrix that transforms a vector in background space to observational space. Assuming 1) $\vec{x}^b = \vec{x}^t + \vec{e}^b$ with $\vec{e}^b \sim N(0, P^b)$, 2) $\vec{y}^o = H\vec{x}^t + \vec{e}^o$ with $\vec{e}^o \sim N(0, R^o)$, 3) $\vec{x}^a = G\vec{x}^b + K\vec{d}^{ob} = \vec{x}^t + \vec{e}^a$, where $\vec{e}^a \sim N(0, P^a)$, one can find matrix $G = I$, $K = P^bH^T(HP^bH^T + R^o)^{-1}$, is the solution that minimizes the trace of $P^a = E(\vec{e}^a\vec{e}^{aT})$ with the constraint $E(\vec{e}^a) = \vec{0}$.

3.2 Implementation

1) x^t with time step 0.01 is generated by integrating and sub-sampled with a time window of 0.1.
2) $y^o(t) = Hx^t(t) + \sigma^o * N(0,1)$
3) choose $\vec{x}^b(0) = \vec{x}^a(0) = \vec{x}^t(0) + \sigma^n * N(0,1)$.
4) choose P^b =diagonal matrix with σ_b^{i2} on the diagonal and $R^o = \sigma^{o2} * I_{L\times L}$, where L is the dimension of $\vec{y}^o$.
5) calculate $K^{oi} = P^bH^T(HP^bH^T + R^o)^{-1}$
6) For t=0:T*TW:

$$\begin{aligned} \vec{x}^b(t+TW) &= \text{integrate 10 steps forward from } \vec{x}^a(t) \text{ using RK4} \\ \vec{d}^{ob}(t+TW) &= \vec{y}^o(t+TW) - H\vec{x}^b(t+TW) \\ \vec{x}^a(t+TW) &= \vec{x}^b(t+TW) + K^{oi}\vec{d}^{ob}(t+TW) \end{aligned}$$

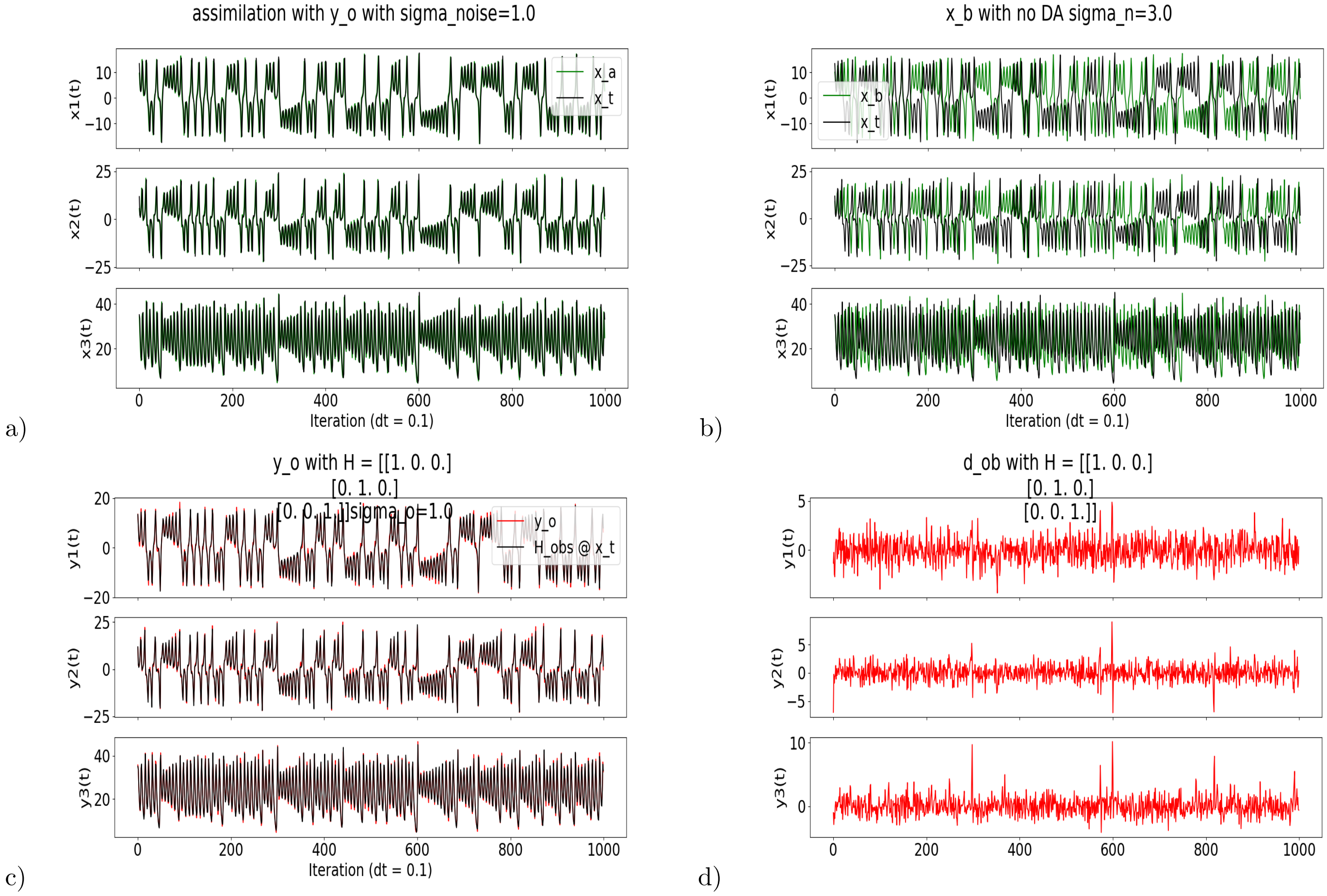

Figure 1: a) analysis when full state is observed using OI, with a MSE=0.4209 b) background when no DA is applied, with a MSE=140.2391 c) observation with noise $\sigma_o = 1.0$ d) Innovation over time

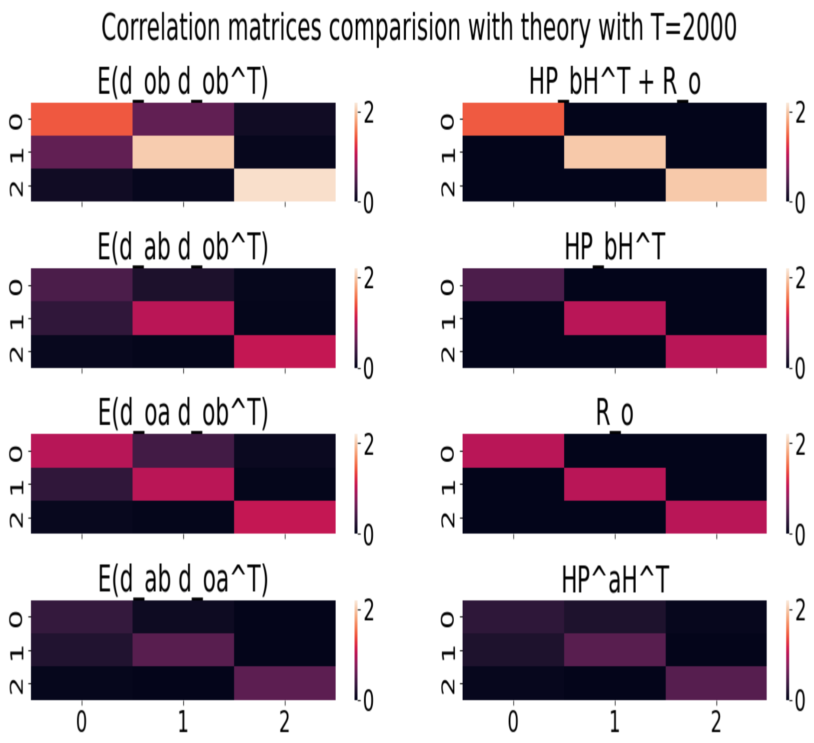

Figure 2: comparing calculated expected value of correlation matrices on the left with corresponding theoretical value on the right

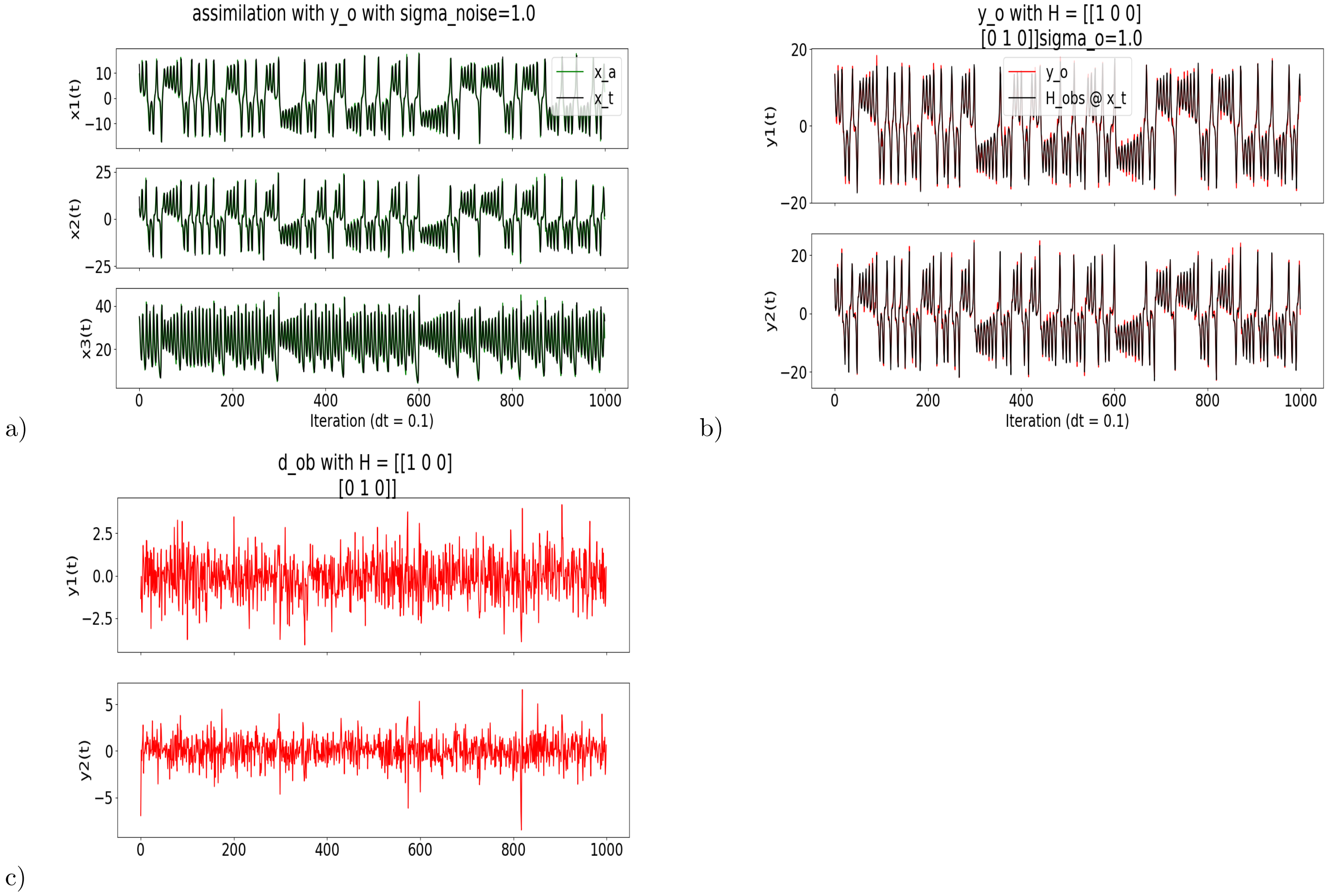

Figure 3: a) analysis when only x and y is observed using OI, with a MSE=0.6011 c) observation with noise $\sigma_o = 1.0$ d) Innovation over time

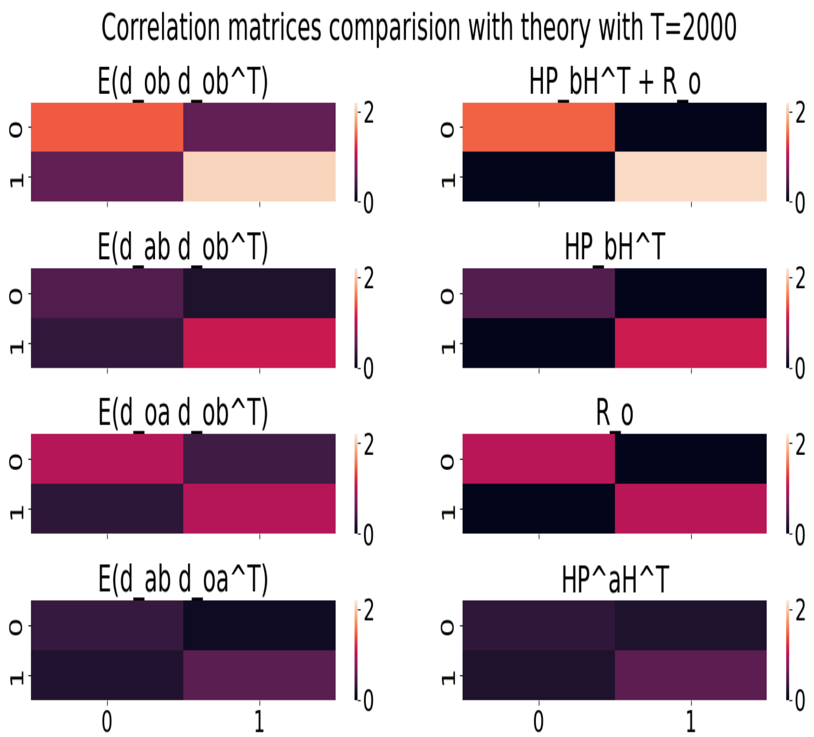

Figure 4: comparing calculated expected value of correlation matrices on the left with corresponding theoretical value on the right

3.3 Results and Validation for OI

Figure 1 shows the results when full states is observed with an observational noise $\sigma^o = 1.0$. The initial background noise $\sigma^n = 3.0$. The P^b is chosen such that $\sigma_b^{x_1 2} = 0.44$,$\sigma_b^{x_2 2} = 1.0$,$\sigma_b^{x_3 2} = 1.0$ is on the diagonal. P^b is tuned by trying to match the $E(\vec{d}^{ob}\vec{d}^{obT})$ matrix to $HP^bH^T + R^o$. starting from using $P^b = 3.0 * I_{3\times3}$, then, $E(\vec{d}^{ob}\vec{d}^{obT})$ over 2000 TW is calculated. The new P^b is adjusted such that $\sigma_b^{x_i 2} = E(d_{ob}^{x_i 2}) - R^{ox_i}$ This is then repeated using the new P^b. After two iterations,the aforementioned values are reached.
It is known from Desroziers et al. [1] such that to achieve optimal linear analysis, the following relationships should hold : 1) $E(\vec{d}^{ab}\vec{d}^{obT}) = HP^bH^T$, 2) $E(\vec{d}^{oa}\vec{d}^{obT}) = R$, 3) $E(\vec{d}^{ob}\vec{d}^{obT}) = HP^bH^T + R^o$, and 4) $E(\vec{d}^{ab}\vec{d}^{oaT}) = HP^aH^T$, with $\vec{d}^{ab} = H(\vec{x}^a - \vec{x}^b)$,$\vec{d}^{oa} = \vec{y}^o - H\vec{x}^a$,$\vec{d}^{ob} = \vec{y}^o - H\vec{x}^b$. These relationships holds as shown in Figure 2. Figure 3 and Figure 4 tell a similar story comparing to Figure 1 and Figure 2, however, the assimilation is done with observing only x and y variables, and no z variable. The P^b is tuned using a similar process, and the value of $\sigma_b^{x_1 2} = 0.47$,$\sigma_b^{x_2 2} = 1.10$,$\sigma_b^{x_3} = 1.0$ is reached.

4 4-D Method : Extended Kalman Filter (EKF)

4.1 Method Description

This approach is similar to the OI approach, however, The P^b is not prescribed with a fixed value over time. The P^b is integrated along with x^b, using the system of equation:

$$\begin{cases} \frac{d\vec{x}^b}{dt} = f(\vec{x}) \\ \frac{dP^b}{dt} = F(\vec{x}^b)P + P^T F(\vec{x}^b)^T + Q \end{cases} \tag{2}$$

Where $F(\vec{x}^b)$ is the tangent Linear Model of Lorenz, which is

$$\begin{pmatrix} -\sigma & \sigma & 0 \\ \rho - z & -1 & -x \\ y & x & -\beta \end{pmatrix}$$

The P^b is also assimilated to P^a with $P^a(t) = (I - K^{oi}(t)H)P^b(t)$ at the end of each time window. Notice that K^{oi} is also changing with time, since P^b is not fixed.

4.2 Implementation

1) x^t with time step 0.01 is generated by integrating and sub-sampled with a time window of 0.1.
2) $y^o(t) = Hx^t(t) + \sigma^o * N(0, 1)$
3) choose $\vec{x}^b(0) = \vec{x}^a(0) = \vec{x}^t(0) + \sigma^n * N(0, 1)$.
4) choose $P^a(0) = P^b(0)$ =diagonal matrix with $\sigma_b^{i^2}$ on the diagonal and $R^o = \sigma^{o2} * I_{L\times L}$, where L is the dimension of $\vec{y}^o$, Q = diagonal matrix with $\sigma_q^{i^2}$ on the diagonal
5) calculate $K^{oi}(0) = P^b(0)H^T(HP^b(0)H^T + R^o)^{-1}$
6) For t=0:T*TW:

$$\begin{aligned} \vec{x}^b(t+TW), P^b(t+TW) &= \text{integrate 10 steps forward from } \ \vec{x}^a(t) \text{ and } P^a(t) \text{ using RK4} \\ \vec{d}^{ob}(t+TW) &= \vec{y}^o(t+TW) - H\vec{x}^b(t+TW) \\ K^{oi}(t+TW) &= P^b(t+TW)H^T(HP^b(t+TW)H^T + R^o)^{-1} \\ \vec{x}^a(t+TW) &= \vec{x}^b(t+TW) + K^{oi}\vec{d}^{ob}(t+TW) \\ P^a(t+TW) &= (I_{3\times3} - K^{oi}(t+TW)H)P^b(t+TW) \end{aligned}$$

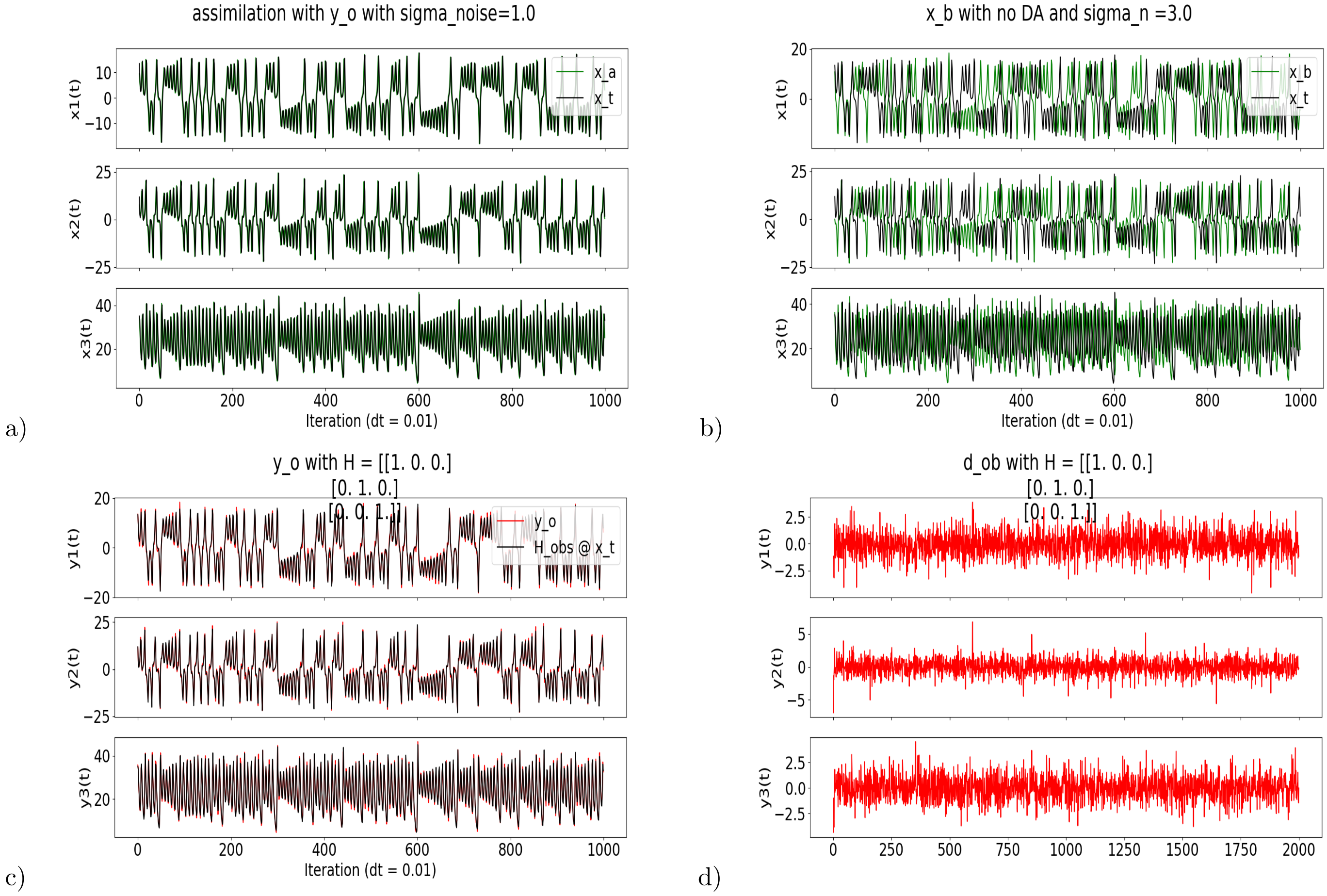

Figure 5: a) analysis when full state is observed using EKF, with a MSE=0.1260 b) background when no DA is applied, with a MSE=148.1618 c) observation with noise $\sigma_o = 1.0$ d) Innovation over time

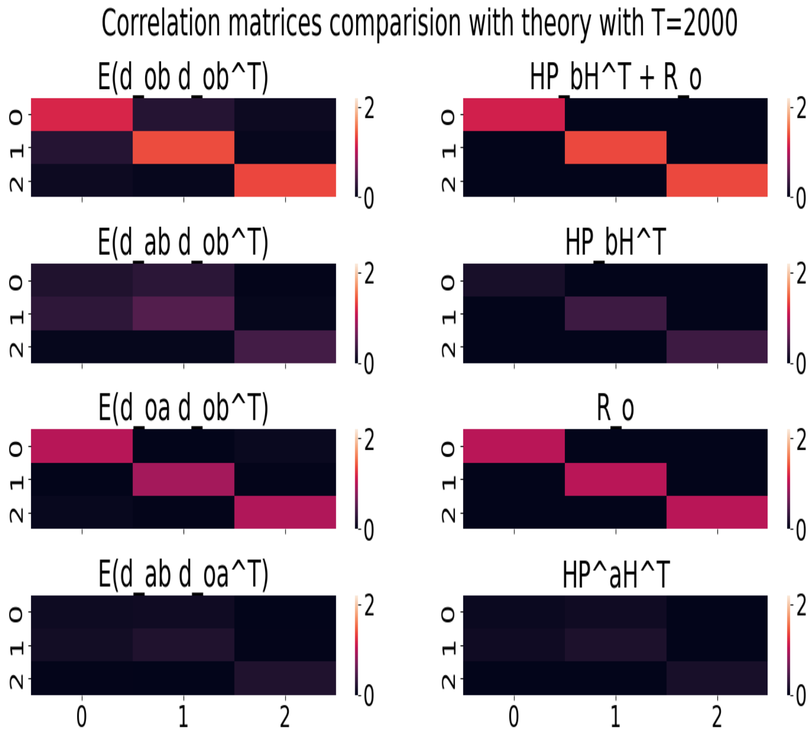

Figure 6: comparing calculated expected value of correlation matrices on the left with corresponding theoretical value on the right

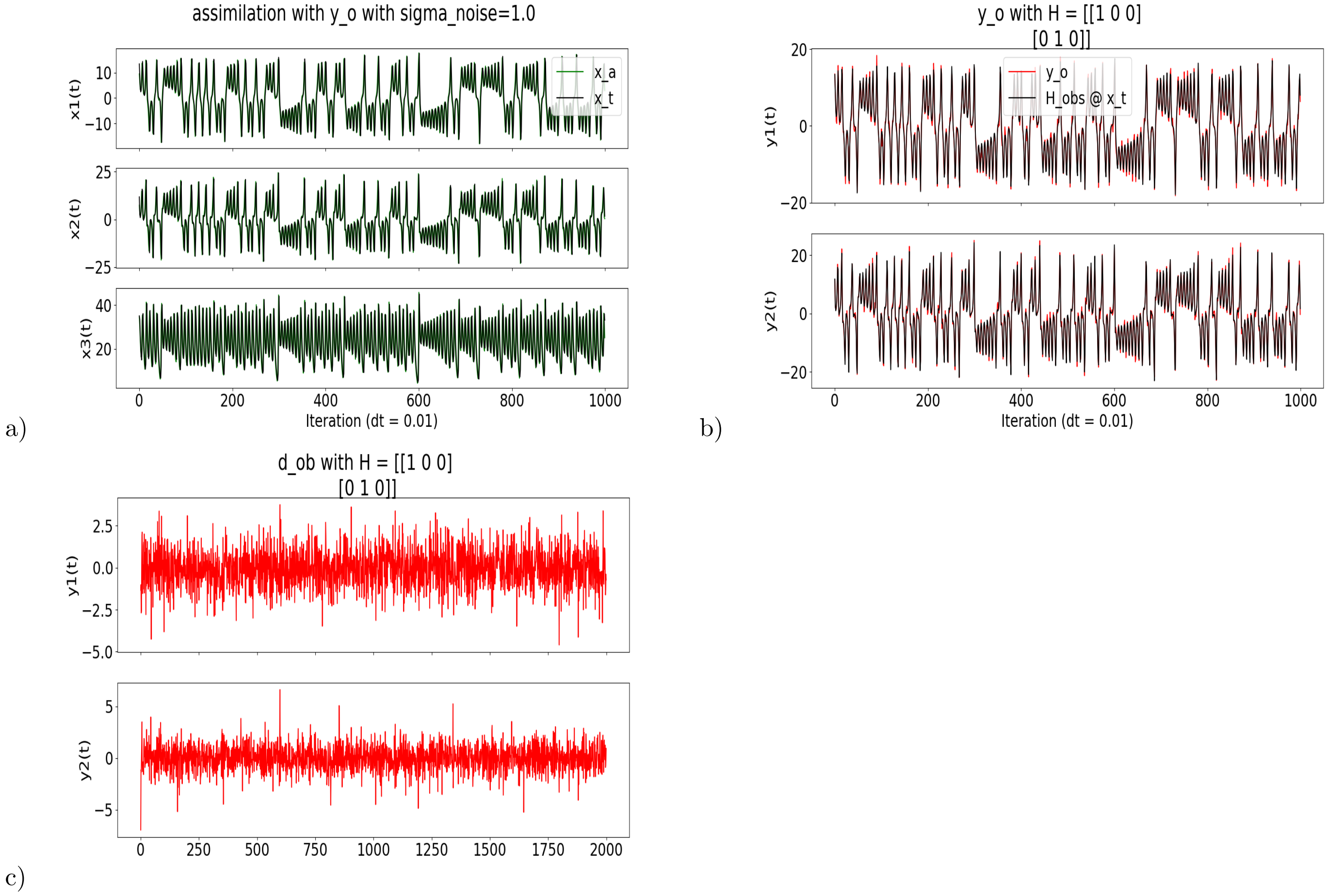

Figure 7: a) analysis when only x and y is observed using EKF, with a MSE=0.2125 c) observation with noise $\sigma_o = 1.0$ d) Innovation over time

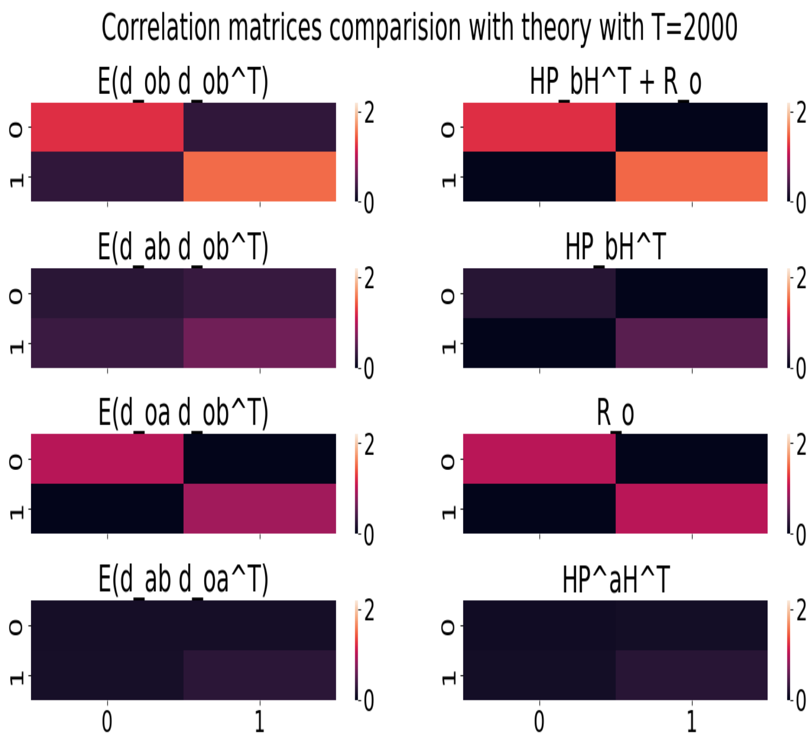

Figure 8: comparing calculated expected value of correlation matrices on the left with corresponding theoretical value on the right

4.3 Results and Validation for EKF

The EKF is tuned with a similar way as OI, the only difference is that instead of tuning P^b as a fixed parameter, $P^b(0)$ and Q is tuned, to match $E(\vec{d}^{ob}\vec{d}^{obT}) = HP^b(0)H^T + R^o$. When full state is observed, the $P^b(0)$ and Q are tuned to a diagonal matrix with $\sigma_b^{x_1 2} = \sigma_q^{x_1 2} = 0.14$,$\sigma_b^{x_2 2} = \sigma_q^{x_2 2} = 0.36$,$\sigma_b^{x_3 2} = \sigma_q^{x_3 2} = 0.36$. When z variables are not observed,the $P^b(0)$ and Q are tuned to a diagonal matrix with $\sigma_b^{x_1 2} = \sigma_q^{x_1 2} = 0.23$,$\sigma_b^{x_2 2} = \sigma_q^{x_2 2} = 0.5$,$\sigma_b^{x_3 2} = \sigma_q^{x_3 2} = 0.36$. Figure 5-8 show similar results as in OI. Notice that for both when full state is observed and when z is not observed, MSE of EKF is smaller than that of OI.

4.4 Validity of Tangent Linear Model

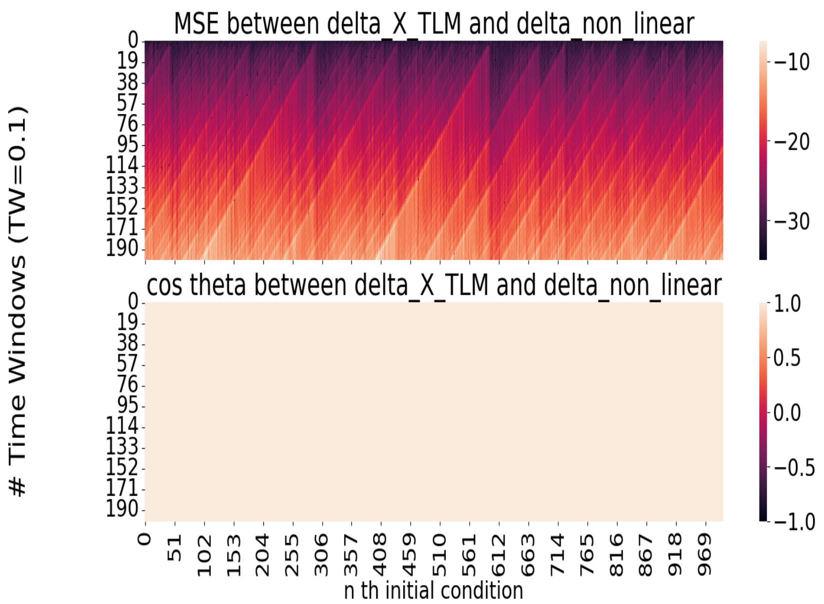

Figure 9: comparing $\delta\vec{x}_{TLM}$ with $\delta\vec{x}_{non-linear}$ over 1000 initial conditions and a run of 200 TW for each condition. The top is log base 10 of mean-squared error(MSE) between the two $\delta x = log_{10}(||\delta\vec{x}_{TLM}(t) - \delta\vec{x}_{non-linear}(t)||^2/3 \text{ dimensions} + 10^{-35})$.The 10^{-35} is added to prevent some taking log of a number that is too close to 0. The maximum MSE between the two $\delta\vec{x}$ is $3.5853 * 10^{-8}$ after 200 TW run. The bottom is the cosine between the vectors, and it is effectively 1 for all the trials.

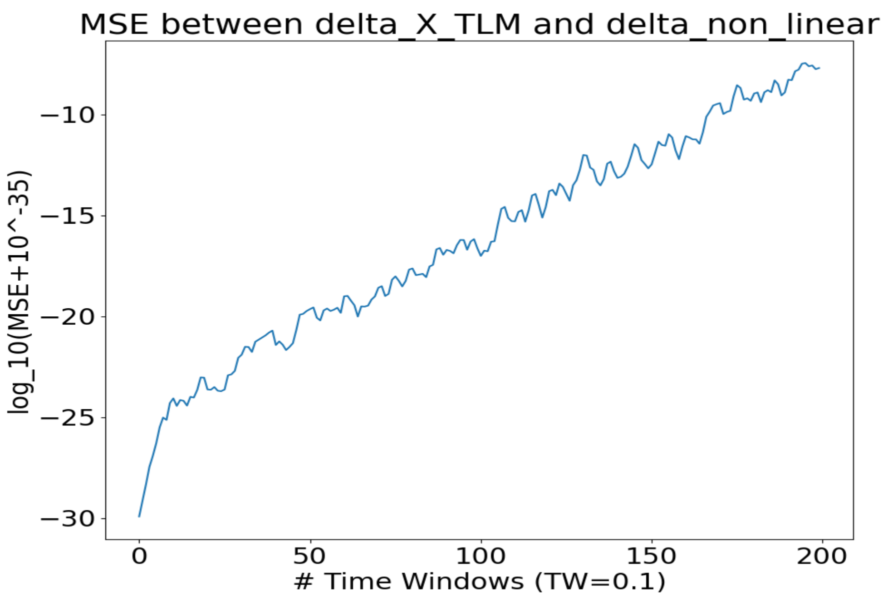

Figure 10: log_{10}(max MSE calculated at t over 1000 initial conditions). There appear to be a exponential law, that $MSE \sim 10^{ct}$, where c is a fixed constant

To verify tangent linear model, the perturbation growth δx is calculated in two algorithms. Starting from introducing a perturbation by adding $\vec{\epsilon} \sim N(0,1)$, to $\vec{x}(0)$ so that $\delta\vec{x}(0) = \vec{\epsilon}$, algorithm one evolves the transfer matrix M from the initial condition $M = I_{3\times3}$ with the equation

$$\begin{cases} \frac{d\vec{x}}{dt} = f(\vec{x}) \\ \frac{dM}{dt} = F(\vec{x})M \end{cases} \tag{3}$$

to get $M(t)$, and $\delta\vec{x}_{TLM}(t) = M\delta\vec{x}_{TLM}(0)$; algorithm two evolves $\delta\vec{x}$ directly with the equation

$$\begin{cases} \frac{d\vec{x}}{dt} = f(\vec{x}) \\ \frac{d\delta\vec{x}_{non-linear}}{dt} = F(\vec{x})\delta\vec{x}_{non-linear} \end{cases} \tag{4}$$

to get $\delta x_{non-linear}(t)$. If the tangent Linear model F is working correctly, these two ways of getting $\delta\vec{x}(t)$ should have similar results. In figure 9, the MSE between the two $\delta\vec{x}$ and the cos angle between them is plotted. 1000 initial conditions, which span over 100 Lyapunov times of data are investigated, which should reach ergodicity. Even after t=200 TW (20 Lyapunov time), the two $\delta\vec{x}$ has only a MSE of $3.5853 * 10^{-8}$. The cosine angles between the two $\delta\vec{x}$ is very close to 1 for all trails. Further trials shows that this MSE grows to O(1) in 300 TW. Figure 10 shows that the maximum MSE between the two $\delta\vec{x}$ over all initial conditions is growing exponentially with a fixed exponent. If a line is drawn continuing from the end point of this log plot at TW=200 with the same slope, it is expected that the MSE will reach O(1) at 300 TW. The integration step is 0.01, which is much smaller than 300 TW=30, and in that time interval, the tangent linear model approximation is valid.

4.5 Is P^a and P^b Positive Definite and Symmetric ?

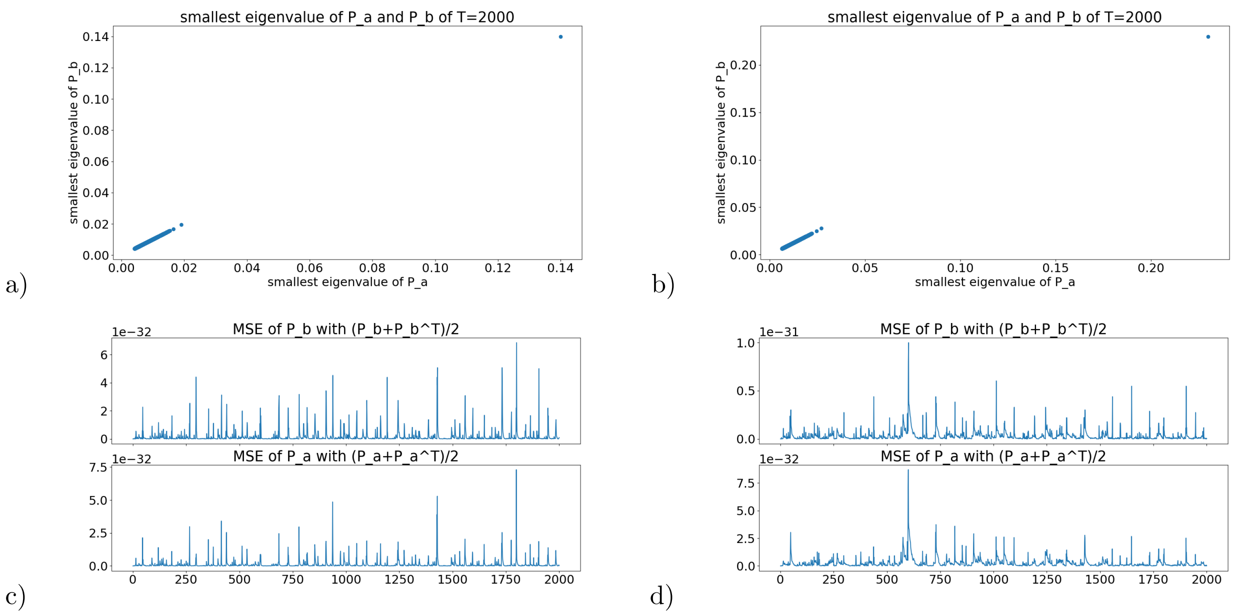

Figure 11: a)scatter plot of the smallest eigenvalues of $P^b(t)$ vs that of $P^a(t)$ when full state is observed. b) scatter plot of the smallest eigenvalues of P^b vs that of P^a when only x and y is observed. c) The MSE between $P^a(t)$ and $(P^a(t) + P^{aT}(t))/2$ and $P^b(t)$ and $(P^b(t) + P^{bT}(t))/2$ for 2000 TW when full state is observed,d) same MSEs as in c), but when only x and y is observed

Figure 11 a and b show the scatter plots of the smallest eigenvalues of $P^a(t)$ and that of $P^b(t)$; it is clear that for both full state and no z observation cases, the $P^a(t)$ and $P^b(t)$ have non-negative eigenvalues. Thus, these matrices are positive definite. Figure 11 c) and d) compare both $P = P^b(t)$ and $P^a(t)$ with the symmetrized version $(P + P^T)/2$. For symmetric matrices, $P = (P + P^T)/2$. The plots shows that the MSE between P and $(P + P^T)/2$ is on the order of 10^{-31}, which is around matrix multiplication precision squared. The precision for matrix multiplication in numpy for a float 64 number is around 10^{-16}, and any number smaller than that has rounding error [2]. So both $P^a(t)$ and $P^b(t)$ should be considered symmetric.

4.6 Comparing $\vec{d}^{oa}$ to $\vec{d}^{ob}$

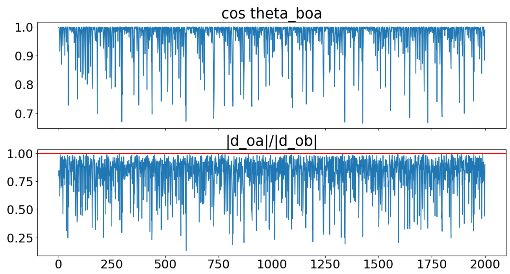

a)

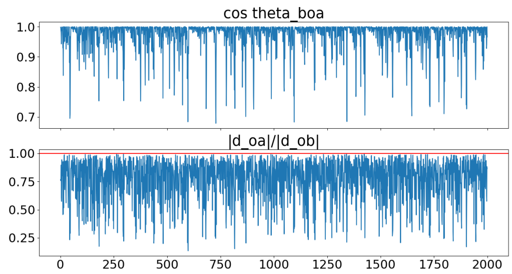

b)

Figure 12: cos of the angle between $\vec{d}^{ob}$ and $\vec{d}^{oa}$,which is expected to be greater than 0 b) ratio of magnitude of $\vec{d}^{oa}$ and $\vec{d}^{ob}$ which is expected to be less than 1 for a) the fully observed case and b) the no Z observed case

According to a paper by Desroziers et al,[1] the ratio of magnitude of the distance between background and analysis from observation $|\vec{d}^{oa}|/|\vec{d}^{ob}| < 1$, and the cosine angle between them should be positive. Figure 12 shows that both of these assumptions hold.

5 Discussion and Future Work

For all trials, EKF has a smaller MSE compared to OI, and thus, having a P^b that is inflated throughout time is better than a fixed P^b. In the tuning process for both OI and EKF, only the diagonal P^b or Q is considered. However, from Figure 2 and Figure 4, it is clear from the calculated $E(\vec{d}^{ob}\vec{d}^{obT})$ that there could be non-zero diagonal elements. Thus, when computing resources allow, a grid search should be conducted to iterate over a range of symmetric P^b or Q to compare for the best parameter.

6 Data Availability

All data and plots are available on https://github.com/Shanlovescode/AOSC_615

References

[1] G. Desroziers et al. "Diagnosis of observation, background and analysis-error statistics in observation space". In: *Quarterly Journal of the Royal Meteorological Society* 131.613 (2005), pp. 3385–3396. DOI: https://doi.org/10.1256/qj.05.108. eprint: https://rmets.onlinelibrary.wiley.com/doi/pdf/10.1256/qj.05.108. URL: https://rmets.onlinelibrary.wiley.com/doi/abs/10.1256/qj.05.108.

[2] Numpy developer. *Data Types*. URL: https://numpy.org/doc/stable/user/basics.types.html.

[3] Ross N. Hoffman and Robert Atlas. "Future Observing System Simulation Experiments". In: *Bulletin of the American Meteorological Society* 97.9 (2016), pp. 1601–1616. DOI: 10.1175/BAMS-D-15-00200.1. URL: https://journals.ametsoc.org/view/journals/bams/97/9/bams-d-15-00200.1.xml.

[4] Edward N. Lorenz. "Deterministic Nonperiodic Flow". In: *Journal of Atmospheric Sciences* 20.2 (1963), pp. 130–141. DOI: 10.1175/1520-0469(1963)020⟨0130:DNF⟩2.0.CO;2. URL: https://journals.ametsoc.org/view/journals/atsc/20/2/1520-0469_1963_020_0130_dnf_2_0_co_2.xml.